Generic Model of PEM Fuel Cells and Performance Analysis in Frequency Containment Period in Systems with Decreased Inertia

F.A. Alshehri[1], J.L. Rueda Torres[1*], A. Perilla[1], B.W. Tuinema[1], M.A.M.M. van der Meijden[1,2], Peter Palensky[1], F. Gonzalez-Longatt[3]

[1]Intelligent Electrical Power Grids, Delft University of Technology, Delft, The Netherlands

[2]TenneT TSO B.V., Arnhem, The Netherlands

[3]Centre for Renewable Energy Systems Technology (CREST), Loughborough University, United Kingdom

*J.L.RuedaTorres@tudelft.nl

***Abstract*— The increase in renewable energy sources in addition to the decrease in conventional synchronous generators is leading to significant challenges for the power system operators to maintain generation load balance and to manage the system's decreasing inertia. Proton Exchange Membrane (PEM) fuel cells are characterised by high current density and fast power injection, which makes them ideal for frequency containment. This paper presents a generic model for PEM fuel cells developed in PowerFactory for frequency stability studies and provides an evaluation of its performance in a reduced-size dynamic model of the North Netherlands high voltage transmission network. The results show that the PEM fuel cell provides improved frequency response within the containment period when compared with synchronous generators for the same amount of support reserve.**

Index Terms--frequency response, fuel cells, renewable energy sources, power system stability.

I. INTRODUCTION

The increasing share of Renewable Energy Sources (RES) increases the variability of electrical power generation, challenging system operators to maintain balance between generation and demand, which implicitly affects frequency stability. Also, replacing synchronous generators with RES results in decreasing inertia in the system, which can involve high Rate-of-Change-of-Frequency (RoCoF) values due to sudden occurrence of active power imbalance. One of the promising technologies that can support to keep active power balance are electrolysers and fuel cells, because of their high current density and fast response. This paper presents a generic model for Proton Exchange Membrane (PEM) fuel cells, including fuel cell dynamics and power control. The model is used to test the fuel cell ability to provide frequency containment reserve in a system with decreasing inertia.

In literature, several approaches have been adopted to develop the model and characterisation of the steady state and dynamic behaviour of PEM fuel cells. For example, models based on electrochemical equations, [1]-[4], provide valuable insight into the reactions that happen within the stack, yet they are very complex and require the knowledge of technical parameters that are not always publicly available. On the other hand, models based on mathematical approximations, semi-empirical or empirical data and model fitting, [5]-[10], are generally simpler, but they represent specific commercial fuel cells, and thus may not be generalised to all existing units. Unfortunately, none of these models can be used to study the frequency stability of the power system. This paper develops an expanded generic PEM fuel cell model that includes frequency and power control and can be used for frequency stability studies on large scale. The model is then used to evaluate the effectiveness of PEM fuel cells in supporting the frequency stability of the power system.

This paper starts with a description of frequency stability and Frequency Containment Reserve (FCR) in section II. Section III presents a generic dynamic model of the PEM fuel cell. This model is tested in a reduced model of the 380-kV North Netherlands transmission network in section IV. Finally, the conclusions from this work and the outline for future research are presented in section V.

II. FREQUENCY STABILITY

A. Description of Frequency Stability

Frequency stability is defined as the ability of a power system to maintain a steady frequency following a severe system upset resulting in a significant imbalance between generation and load demand [11]. The instability in such case will result in increasing frequency deviation or sustained frequency oscillations. In the case of a severe disturbance that results in a sudden generation-load demand imbalance, the frequency will start to deviate, and the power system response to such deviation is defined in three classifications: inertial response, primary frequency response and secondary frequency response. Inertial response is responsible for resisting frequency changes in the first 5-10 seconds after the disturbance, and it depends on the amount of rotating mass in the system, which is typically associated to synchronous generators. Primary frequency response works to arrest and stabilise the frequency response in the entire connected synchronous area after a disruption during the first 30 seconds [12]. Secondary frequency control acts after primary frequency control in order to restore the active power balance in each control area within 15 minutes after a disturbance.

B. *Frequency Ancillary Services*

In the context of frequency stability, ancillary services are operational reserves that the Transmission System Operator (TSO) can procure to preserve the balance between supply and demand to maintain frequency stability. The service considered in this study is Frequency Containment Reserve (FCR): a market implementation of primary frequency support through an auction platform. The focus of this paper is on PEM fuel cell participation in the FCR market as a supplier. The TSO identifies the required reserve capacity based on the total generation capacity in the managed area, suppliers submit their symmetrical bids, and the lowest bids are chosen until the required reserve capacity is achieved. The suppliers' bids should be activated automatically with frequency deviation and should change the output power through a linear droop control mechanism [13]:

$$\Delta P = P_{bid} \frac{|f - f_0|}{\Delta f_{max}} \quad (1)$$

where ΔP is the change in generator power in MW, P_{bid} is the bid value in MW, f is the measured frequency in Hz, f_0 is the reference frequency in Hz, and Δf_{max} is the full activation frequency deviation, which is the frequency deviation value where the supplier should provide the full bid amount. For example, in the Dutch system, the full activation frequency deviation is 200 mHz, and suppliers can also have a deadband of 10 mHz as illustrated in Fig. 1. A detailed description of the FCR market mechanism is provided in [13], [14].

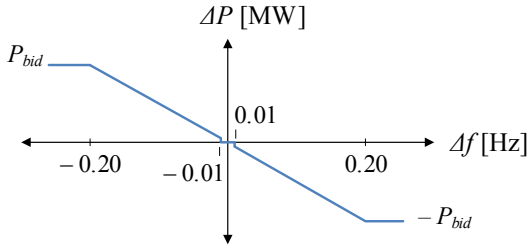

Figure 1. Droop control for FCR suppliers in the Dutch market.

III. PEM Fuel Cell Model

A. *PEM Fuel Cell Model*

In literature, several approaches have been adopted to develop the model and characterisation of the steady-state and dynamic behaviour of PEM fuel cells. Some are based on the electrochemical equations, while some are based on empirical data and model fitting. A comprehensive review of literature models is provided in [15]. In this paper, a generalised model of PEM fuel cells for frequency support applications is developed, which covers the dynamics of the stack, the power conditioning system (i.e. DC-AC inverter) and the balance of plant. The developed model is built upon previous research [16], that estimates physical parameters through experiments and empirical data collection from the 1.2-kW Nexa PEM fuel cell, a frequently studied unit in this field. An advantage of using the Nexa model is the inclusion of an air compressor, a cooling fan and fully automated control [17], making it possible to incorporate the description of the balance of plant within the stack model. This paper builds upon the model from [16] and expands it with a frequency droop controller and active/reactive power control. The performance of this model is then studied in several grid-connected frequency stability studies.

The voltage of the fuel cell stack is dependent on the drawn current and the stack temperature. While the load determines the current, the temperature can be defined through a thermodynamic model. In order to simplify the modelling of the fuel cell, it will be assumed that the gases are ideal and uniformly distributed, gas flow will be at constant pressure at both anode and cathode, individual fuel-cell stacks can be lumped together to represent the fuel-cell array, and thermodynamic. The parameters of the developed fuel cell model are estimated using empirical data, which results in a very close fit to experimental measurements.

The following equation can represent the dynamic model for temperature change [16]:

$$T(t) = T_2 + (T_1 - T_2) \times \exp\left(-\frac{\mathrm{H_t}}{mc_p} t\right) \quad (2)$$

where T_1 is the initial temperature, T_2 is the final steady state asymptotic temperature, H_t is the heat transfer coefficient (W/°C) and mc_p is the thermal capacitance (J/°C). The fuel cell output voltage as a function of current is empirically defined by the following equation [18]:

$$V = E_0 - IR - A \ln\left(\frac{I}{I_{ex}}\right) \quad (3)$$

where E_0 is the Nernst potential in Volts, R is the resistance in ohms, A is the Tafel Slope in Volts and I_{ex} is the exchange current in amperes, which is considered a constant. The Nernst potential is calculated by [19]:

$$E_0 = 47 \times \begin{bmatrix} 1.482 - 0.000845 T_K + \\ 0.0000431 T_K \, ln\left(p_{H_2} p_{O_2}^{0.5}\right) \end{bmatrix} \quad (4)$$

where T_K is the stack temperature in Kelvin and $p_{\mathrm{H_2}}, p_{\mathrm{O_2}}$ are the hydrogen and oxygen pressures in atm, respectively. Multiplication by 47 is to account for the 47 individual cells within the stack. The other parameters are estimated using empirical data fitting. The resistance is dependent on the temperature and is defined as [16]:

$$R(T_K) = R_0 \times exp\left(\frac{E_{a,R}}{R_g T_K}\right) \quad (5)$$

where R_0 is the pre-exponential factor in ohms and $E_{a,R}$ is the activation energy in J/mol. The Tafel slope is also dependent on temperature and is defined as [16]:

$$A(T_K) = A_0 \times \exp\left(\frac{E_{a,A}}{R_g T_K}\right) \quad (6)$$

where A_0 is the pre-exponential factor in Volts and $E_{a,A}$ is the activation energy in J/mol. The output power from the fuel cell is simply the multiplication of the output current and the stack voltage. Table I gives the parameters for the fuel cell dynamic model equations.

TABLE I. PARAMETERS FOR FUEL CELL DYNAMIC MODEL EQUATIONS

Parameter	Value and Unit	Equation
mc_p	4304 J/°C	2
H_t	$15.07 \times I^{0.2358}$ W/°C	2
I_{ex}	1×10^{-6}A	3
R_0	0.1537 Ω	5
$E_{a,R}$	1800 J/mol	5
A_0	0.1591 V	6
$E_{a,A}$	5344 J/mol	6

The use of per unit inputs and outputs for the dynamic model makes the developed model generic and can, therefore, be used to represent any size of fuel cell.

B. *PowerFactory Model*

The fuel cell is represented in PowerFactory through the static generator built-in component, configured to perform as an externally controlled current source. In PowerFactory, the static generator is used to represent any type of non-rotating generator connected to the grid via a converter. The control of the static generator is developed using DIgSILENT Simulation Language (DSL), which can be programmed using visual structures such as frames and blocks. The model can be divided into three parts as shown in Fig. 2.

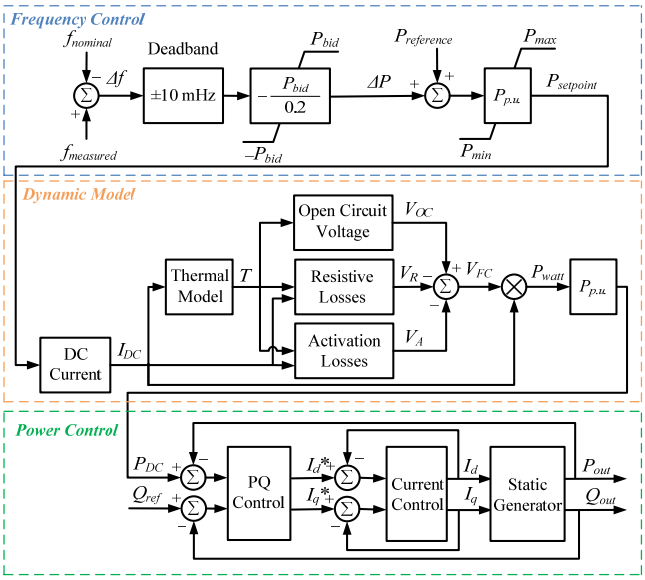

Figure 2. Dynamic model for PEM fuel cell for Frequency Containment.

The frequency control measures the frequency deviation and applies a deadband, e.g. 10 mHz for the Dutch system. Then, the signal is run through a droop control block which is defined by the following equation:

$$\Delta P = -P_{bid} \frac{(f - f_{nominal})}{Full\ Bid\ Frequency\ Deviation} \quad (7)$$

where P_{bid} is the bid value as decided by the FCR market in MW, f is the measured frequency in Hz, $f_{nominal}$ is the reference frequency in Hz and *Full Bid Frequency Deviation* is the frequency at which the generator shall supply the full bid value and it is decided by the system operator, e.g. 200 mHz for the Dutch system. The power output of this block (ΔP) is limited by the value of the bid (P_{bid}) and does not exceed it, even if the frequency deviation goes beyond the full bid frequency deviation. The power reference is then added in order to give the power setpoint for the fuel cell, which is converted to per unit. Limits are applied to the power setpoint to ensure that the fuel cell plant operates within the allowable limits, i.e. 20–100% of the fuel cell plant rated power.

The dynamic model converts the incoming power setpoint from the frequency control to Watt by multiplying by the rated power of the Nexa Fuel cell. Then, the current drawn (i.e. DC intensity in Ampere) is calculated using empirical data from [17], which is implemented as a look-up table. The current is fed into the next block, which represents the thermal model from (2). In the equation, the initial and final asymptotic temperatures are calculated using empirical data from [16], which is implemented as a look-up table as well. The current and temperature signals are then fed into the next three parallel blocks, which represent the open circuit voltage in (4), the resistive losses in (5) and the activation losses in (6), respectively. The outputs of these blocks are added in order to give the instantaneous stack voltage, which is multiplied by the current to give the output power of the fuel cell in Watt. This is converted into per unit by dividing by the fuel cell rated power.

The power control consists of two loops: an outer power control loop that controls the active power (P_{out}) and reactive power (Q_{out}), and an inner current control loop that controls the currents I_d and I_q in the synchronous reference frame as shown in Fig. 3.

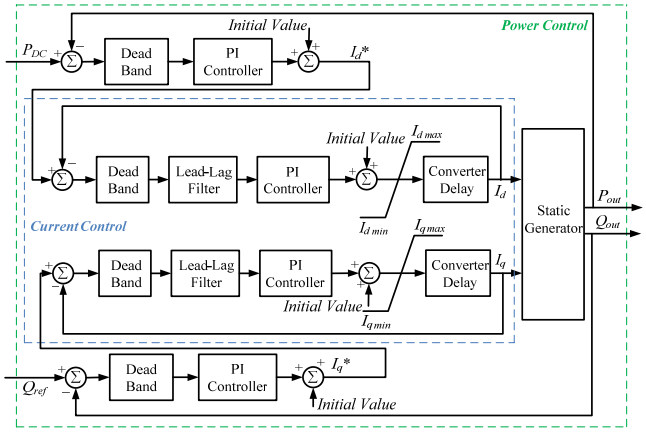

Figure 3. Fuel cell power and current control loops.

For *P*-control, the output power is compared with the reference power signal from the dynamic model, and applied through a deadband filter, and then into a Proportional-Integral (PI) controller. An initial value is added which gives the setpoint I_d^*. This setpoint is compared against the actual measured value of I_d, and the result is fed through a deadband and a lead-lag filter, and then into a PI controller. The initial value is added, limits are applied, and a small converter delay is added. The output signal is fed into the

static generator, which supplies P and Q to the grid. Q-control is identical, except that reactive power is controlled to remain constant throughout the operation of the fuel cell.

C. Model Validation

The accuracy of the developed model was tested against other models in the literature. First, by using (2)-(6), the stack voltage was calculated for each output current value from 0 to 45 A and compared to literature values from [20]. Fig. 4 shows the literature data and the model output. The data shows close resemblance for static operation. There is some offset for low values of current; however, since the fuel cell will be operated at minimum 20%, this offset is not of concern as long as the model shows a resemblance of linear behaviour at higher current values.

The dynamic part of the PowerFactory model is compared with experimental data from [21], and the results shown in Fig. 5 are due to several step changes in drawn current. Comparison of the data shows an almost identical output. The exception is at a low current, which is at low power, where the voltage level is different. However this issue does not affect the reliability of the dynamic model, since at a current less than 9 A, the power output is beyond the normal operating range of 20-100%.

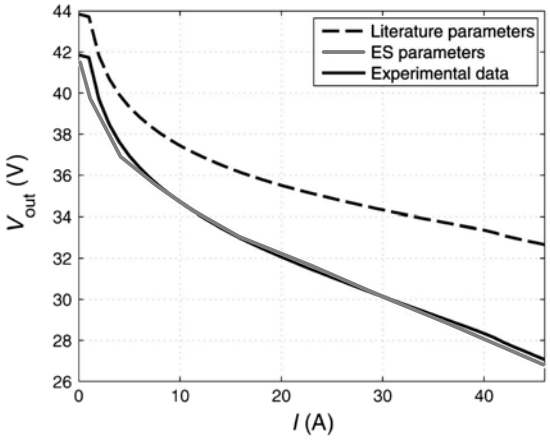

(a) Literature data [20].

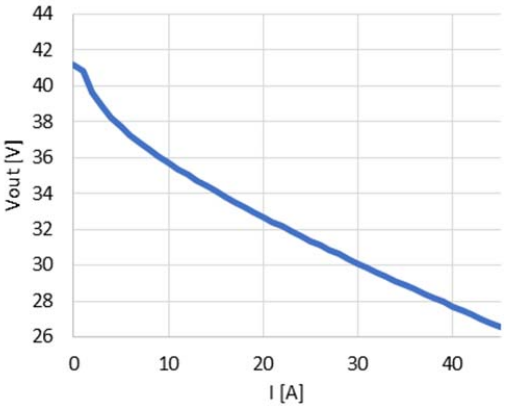

(b) Model output.

Figure 4. Validation of static model output.

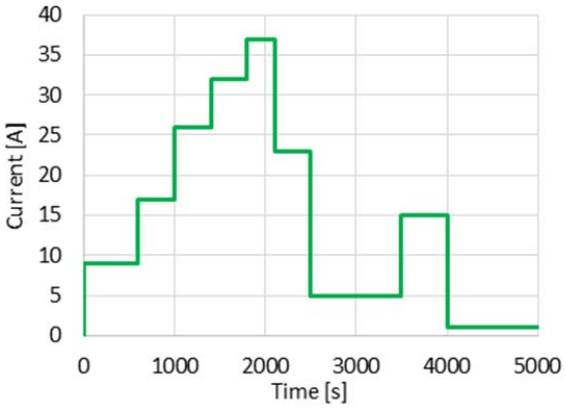

(a) Literature data [21].

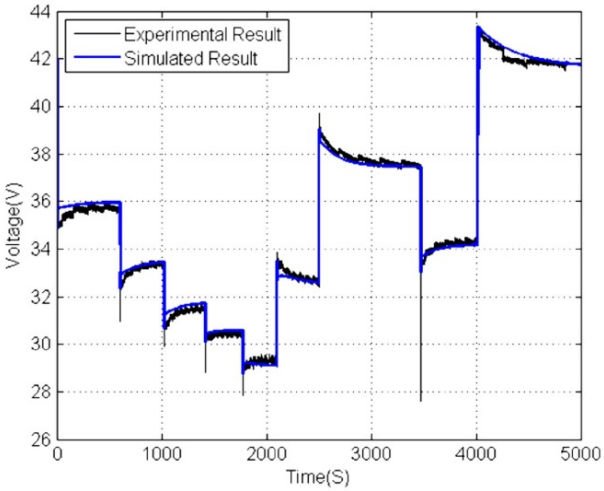

(b) Literature data [21].

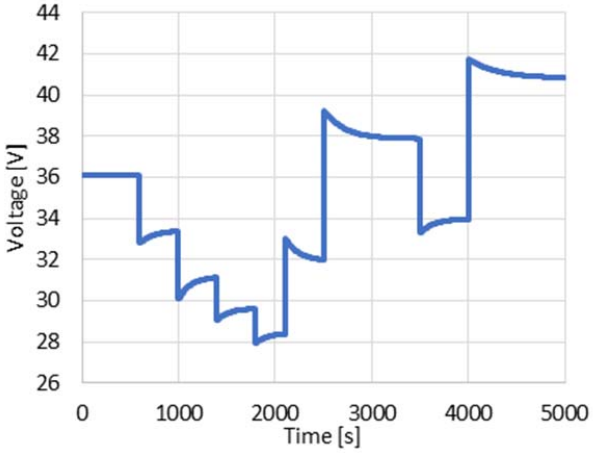

(c) Model output.

Figure 5. Validation of PowerFactory dynamic model output.

IV. Simulation of Frequency Support

The fuel cell is tested for its availability to support the frequency by using a reduced representation of the 380-kV Northern Netherlands grid as shown in Fig. 6. This model consists of the 380-kV transmission network of the northern provinces of the Netherlands, together with some 220-kV transmission lines and substations. This part of the power system is particularly suitable for this particular study as it includes a combination of conventional generation, large-scale offshore wind and submarine interconnections, while the exploitation of Power-to-Gas in this area is foreseen for the future. The Northern Netherlands grid features two synchronous generators (at EOS), one offshore wind farm (Gemini), two HVDC links (COBRAcable and NorNed), and multiple onshore wind farms distributed around the area.

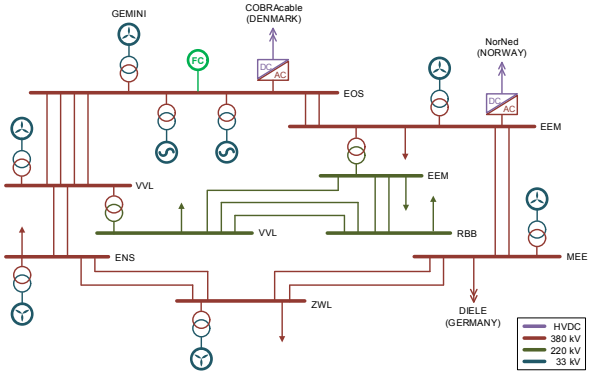

Figure 6. North Netherlands test network.

The simulated disturbance is a decrease in wind generation of 30 MW at $t = 5$ s at the bus EEM, which creates an imbalance between generation and load causing significant frequency deviation and dramatic values for the Rate-of-Change-of-Frequency (RoCoF). In this system, the inertia is only provided by the synchronous generators, and it is calculated by summing the inertia constants of the synchronous generators. The FCR support is provided only through the synchronous generators, the fuel cells, or both.

The disturbance is simulated for several scenarios with different FCR contributions from the synchronous generators and the fuel cells, for a decreasing level of inertia. The system inertia is reduced by reducing the inertia constant of the synchronous generators. A list of these scenarios and a summary of the frequency response are provided in Table II, while the frequency response is shown in Fig. 7.

The results of the simulation in Fig. 7 show that for the same FCR bid value and the same system inertia, the PEM fuel cells result in better frequency nadir, smaller oscillations and faster convergence to the steady state value. The improvement in performance becomes more prominent as the system inertia decreases, such as in scenario 4 and 5, in which the faster power injection by the PEM fuel cell is able to contain the frequency deviation quickly resulting in significantly smaller nadir. The oscillations observed in scenario 5 are due to the reduced inertia of the synchronous generators.

TABLE II. Summary of Simulation Scenarios

N°	Scenario	System inertia	FCR bids	Nadir [Hz]	RoCoF [mHz/s]
1	**Base case**	100%	50 MW by SG	49.845	28.575
2	**Full inertia with FC**	100%	50 MW by FC	49.900	28.399
3	**Lowered inertia with FC**	50%	50 MW by FC	49.899	60.138
4	**Min inertia with SG**	25%	50 MW by FC	49.794	122.964
5	**Min inertia with FC**	25%	50 MW by FC	49.894	118.682

* The value of the system inertia for the base case is 10 seconds.
(FC = fuel cells; SG = synchronous generators)

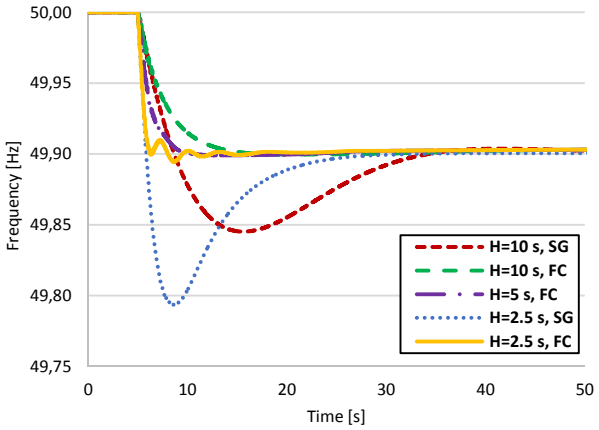

Figure 7. Frequency response of the North Netherlands test network.
(H = system inertia constant; FC = fuel cell; SG = synchronous generator)

V. Conclusions

A representative dynamic model was developed to represent PEM fuel cells in dynamic simulations concerning frequency performance during the containment period. The simulations of the model show that it resembles the expected performance shown in literature. When tested in a reduced representation of the North Netherlands system, fuel cells proved effective in containing the frequency change. A comparison between the PEM fuel cell and synchronous generators performance in frequency containment showed that the fuel cell's fast current injection results in better nadir value and smaller oscillations, however the RoCoF value remains unaffected. Future research can address verifying the results through simulation in other simulation platforms and studying performance of other fuel cell types in frequency containment.

Acknowledgment

This work has received funding from the European Union's Connecting Europe Facility (CEF) programme under the grant agreement No INEA/CEF/SYN/A2016/1336043– TSO Project (Electric "Transmission and Storage Options" along TEN-E and TEN T corridors for 2020). This paper reflects only the authors' views and the European Commission is not responsible for any use that may be made of the information it contains.

Co-financed by the European Union
Connecting Europe Facility

REFERENCES

[1] J. C. Amphlett, R. F. Mann, B. A. Peppley, P. R. Roberge, and A. Rodrigues, "A model predicting transient responses of proton exchange membrane fuel cells," *Journal of Power Sources*, vol. 61, no. 1, pp. 183-188, Jul. 1996.

[2] C. Wang, M. H. Nehrir, and S. R. Shaw, "Dynamic models and model validation for PEM fuel cells using electrical circuits," *IEEE trans. on energy conversion*, vol. 20, no. 2, pp. 442-451, Jun. 2005.

[3] J. Andujar, F. Segura, and M. Vasallo, "A suitable model plant for control of the set fuel cell− DC/DC converter," *Renewable Energy*, vol. 33, no. 4, pp. 813-826, Apr. 2008.

[4] I. San Martín, A. Ursúa, and P. Sanchis, "Modelling of PEM fuel cell performance: Steady-state and dynamic experimental validation," *Energies*, vol. 7, no. 2, pp. 670-700, Feb. 2014.

[5] Y. Hou, Z. Yang, and G. Wan, "An improved dynamic voltage model of PEM fuel cell stack," *International journal of hydrogen energy*, vol. 35, no. 20, pp. 11154-11160, Oct. 2010.

[6] X. Kong, A. M. Khambadkone, and S. K. Thum, "A hybrid model with combined steady-state and dynamic characteristics of PEMFC fuel cell stack," in proc. of *Industry Applications Conference,* 2005. *Fourtieth IAS Annual Meeting.,* Oct. 2005, vol. 3, pp. 1618-1625.

[7] M. V. Moreira and G. E. Da Silva, "A practical model for evaluating the performance of proton exchange membrane fuel cells," *Renewable Energy*, vol. 34, no. 7, pp. 1734-1741, Jul. 2009.

[8] M. Soltani and S. M. T. Bathaee, "Development of an empirical dynamic model for a Nexa PEM fuel cell power module," *Energy Conversion and Management*, vol. 51, no. 12, pp. 2492-2500, Dec. 2010.

[9] C. Restrepo, T. Konjedic, A. Garces, J. Calvente, and R. Giral, "Identification of a proton-exchange membrane fuel cell's model parameters by means of an evolution strategy," *IEEE Transactions on Industrial Informatics*, vol. 11, no. 2, pp. 548-559, Apr. 2015.

[10] P. Gabrielli, B. Flamm, A. Eichler, M. Gazzani, J. Lygeros, and M. Mazzotti, "Modeling for optimal operation of PEM fuel cells and electrolyzers," in proc. of *16th International Conf. on Environment and Electrical Engineering (EEEIC2016)*, Jun. 2016, pp. 1-7.

[11] P. Kundur et al., "Definition and classification of power system stability IEEE/CIGRE joint task force on stability terms and definitions," *IEEE Transactions on Power Systems,* vol. 19, no. 3, pp. 1387-1401,2004.

[12] J. Aho *et al.*, "Tutorial of Wind Turbine Control for Supporting Grid Frequency through Active Power Control," presented at the *American Control Conference (ACC)*, Montreal, QC, 2012.

[13] TenneT Holding B.V. "*Productspecificatie FCR,*" *2015.* [online]. Available: https://www.tennet.eu/fileadmin/user_upload/Bijlage_ B_-_Productspecifications_FCR_ENG.pdf

[14] V. Garcia Suarez, J. Rueda Torres, B. Tuinema, A. Perilla Guerra, and M. van der Meijden, "Integration of Power-to-Gas Conversion into Dutch Electrical Ancillary Services Markets," presented at the *ENERDAY 2018*, Dresden, Germany, 2018.

[15] A. Bıyıkoğlu, "Review of proton exchange membrane fuel cell models," *International Journal of Hydrogen Energy,* vol. 30, no. 11, pp. 1181- 1212, 2005/09/01/ 2005.

[16] H.-i. Kim, C. Y. Cho, J. H. Nam, D. Shin, and T.-Y. Chung, "A simple dynamic model for polymer electrolyte membrane fuel cell (PEMFC) power modules: Parameter estimation and model prediction," *International journal of hydrogen energy,* vol. 35, no. 8, pp. 3656-3663, Apr. 2010.

[17] *Nexa™ Power Module User's Manual*. Ballard Power Systems Inc., 2003.

[18] J. Laramie and A. Dicks, *Fuel cell systems explained*. New York, NY: John Wiley and Sons, 2003.

[19] R. O'hayre, S.-W. Cha, F. B. Prinz, and W. Colella, *Fuel cell fundamentals*. John Wiley & Sons, 2016.

[20] C. Restrepo, T. Konjedic, A. Garces, J. Calvente, and R. Giral, "Identification of a proton-exchange membrane fuel cell's model parameters by means of an evolution strategy," *IEEE Transactions on Industrial Informatics,* vol. 11, no. 2, pp. 548-559, Apr. 2015.

[21] M. Soltani and S. M. T. Bathaee, "Development of an empirical dynamic model for a Nexa PEM fuel cell power module," *Energy Conversion and Management,*" vol. 51, no. 12, pp. 2492-2500, Dec. 2010.